

## Generation of high spectral purity photon-pairs with MgO-doped periodically poled lithium niobate

This content has been downloaded from IOPscience. Please scroll down to see the full text.

2015 Laser Phys. 25 125203

(<http://iopscience.iop.org/1555-6611/25/12/125203>)

View [the table of contents for this issue](#), or go to the [journal homepage](#) for more

Download details:

IP Address: 202.120.14.134

This content was downloaded on 05/11/2015 at 22:05

Please note that [terms and conditions apply](#).

# Generation of high spectral purity photon-pairs with MgO-doped periodically poled lithium niobate

Mengying Zhan, Qichao Sun, Tong Xiang and Xianfeng Chen

The State Key Laboratory on Fiber Optic Local Area Communication Networks and Advanced Optical Communication Systems, Department of Physics and Astronomy, Shanghai JiaoTong University, Shanghai 200240, People's Republic of China

E-mail: [xfchen@sjtu.edu.cn](mailto:xfchen@sjtu.edu.cn)

Received 1 September 2015, revised 22 September 2015

Accepted for publication 6 October 2015

Published 5 November 2015



## Abstract

We study the spectral correlation of photon pairs generated via type-II spontaneous parametric down conversion in periodically poled lithium niobate crystals. By performing Schmidt decomposition on the two-photon wavefunction, we calculate the spectral purity of the two-photon state under various pump laser characteristics and doping concentrations of MgO in lithium niobate crystals. Our results show that periodically poled 5% MgO doped lithium niobate is a good candidate to generate photon-pairs with high spectral purity at telecom wavelength.

Keywords: spectral purity, Schmidt decomposition, spontaneous parametric down conversion

(Some figures may appear in colour only in the online journal)

## 1. Introduction

Interference between quantum states carried by independent photons is vital to the implementation of various entanglement-based protocols such as quantum teleportation [1], entanglement swapping [2], quantum relays [3] and photon amplifiers [4]. To be able to observe interference we have to make sure that the two photons registered behind the beam splitter cannot be distinguished in any way. The widely used technique for generating entangled photon pairs is spontaneous parametric down conversion (SPDC), which can be arranged in diverse configurations and with different crystals [5–7] and waveguides [8, 9]. However, energy conservation ensures that the frequencies of the down-converted photons always sum to the pump frequency, which results in spectral correlations [10]. Because of spectral correlation, it is occasionally possible to identify pairs of photons as siblings [11]. In order to obtain the desired indistinguishability, narrow-band filters are employed to make sure the coherence time of the photon pairs is larger than that of the pump pulses [11]. However, this consequently introduces additional losses, which results in a sharp reduction in the quantity of available photons [12, 13]. Another scheme

is eliminating the spectrum correlation between the photon pairs by adapting the spectrum of the pump pulses and the dispersion property of the nonlinear media. Plenty of previous research has demonstrated that engineering the pump parameters to obtain the photon pairs which are uncorrelated in frequency is feasible. A prime example is spectrally pure photons generated in periodically poled potassium titanyl phosphate (PPKTP). Gerrits *et al* developed a polarisation-entangled source using PPKTP, which produced nearly identical, factorisable frequency modes with 785 nm pump wavelength and 5.35 nm pump bandwidth [14]. In 2014, Bruno *et al*, optimised the phase matching, pump laser characteristics and coupling geometry to acquire spectrally uncorrelated photon pairs with high coupling efficiency [15].

Periodically poled lithium niobate (PPLN) is a typical nonlinear optical crystal, which has been used to generate photon pairs at telecom wavelength for its quite large second-order nonlinear coefficient [16, 17]. The value of the second-order nonlinear coefficient about PPLN with type-II SPDC is  $4.65 \text{ pm V}^{-1}$  and that of PPKTP is  $1.5 \text{ pm V}^{-1}$ . Thus, the quantity of photon pairs generated in PPLN is more than nine times that in PPKTP. Moreover, lithium niobate crystal can

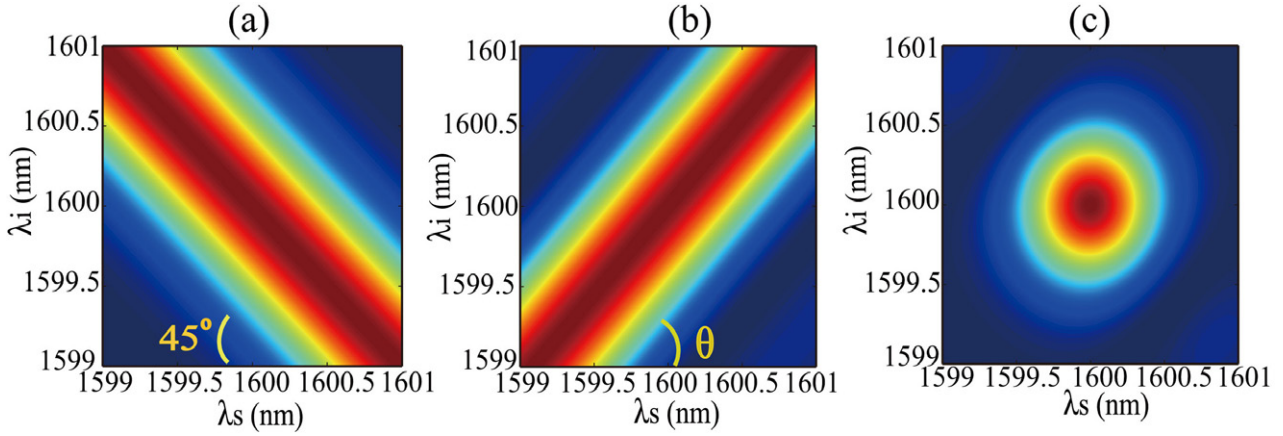


**Figure 1.** Examples of pump envelope intensity  $|\alpha(\omega_s + \omega_i)|^2$  (a), phase matching intensity  $|\phi(\omega_s, \omega_i)|^2$  (b) and JSI  $|f(\omega_s, \omega_i)|^2$  (c).

be doped by magnesium oxide, which not only increases its resistance to optical damage, but also changes its dispersion property [18]. In this paper, we analyse the spectrum purity of the photon pairs generated via SPDC in PPLN with different MgO doping concentrations. According to our calculation, by adjusting the crystal length and the centre wavelength and bandwidth of the pump laser, the 5% MgO doped PPLN can generate photon pairs with a spectral purity of 88%, which is higher than those that can be obtained via PPLN with other doping concentrations.

## 2. Theoretical mode of SPDC

In the process of SPDC, photons from the intense pump beam are occasionally divided into two lower energy photons, the signal and the idler. The correlations between the degrees of freedom of the generated photons are complicated. Here, for simplicity we only consider the frequency part. By using the first-order perturbation theory and the paraxial approximation, the two-photon state of the signal and idler photons can be represented by the following formula:

$$|\varphi\rangle = \int \int d\omega_s d\omega_i f(\omega_s, \omega_i) \hat{a}_s^\dagger(\omega_s) \hat{a}_i^\dagger(\omega_i) |0, 0\rangle, \quad (1)$$

where  $\omega_s$  and  $\omega_i$  are the frequencies of the signal and idler photons,  $\hat{a}_s^\dagger$  and  $\hat{a}_i^\dagger$  represent the creation operators of the signal and the idler fields separately, and the function  $f(\omega_s, \omega_i)$  represents the joint spectral amplitude (JSA), which results from the envelope of the pump energy and phase matching function. It is defined as:

$$f(\omega_s, \omega_i) = N\alpha(\omega_s + \omega_i)\phi(\omega_s, \omega_i), \quad (2)$$

where  $\alpha(\omega_s + \omega_i)$  and  $\phi(\omega_s, \omega_i)$  are the pump envelope amplitude and the phase matching amplitude.  $N$  denotes the normalisation constant. In the nonlinear optical field, the spectrum of the pump laser is considered to have a Gaussian distribution with a bandwidth of  $\sigma_p$ ; therefore, the pump envelope intensity can be written as

$$|\alpha(\omega_s + \omega_i)|^2 = \exp^2 \left[ - \left( \frac{\omega_s + \omega_i - \omega_p}{\sigma_p} \right)^2 \right], \quad (3)$$

where  $\omega_p$  is the frequency of the pump. The phase matching intensity is given by

$$|\phi(\omega_s, \omega_i)|^2 = \left\{ \text{sinc} \left\{ \frac{L}{2} [k_s(\omega_s) + k_i(\omega_i) - k_p(\omega_s + \omega_i)] \right\} \times \exp \left\{ -i \frac{L}{2} [k_s(\omega_s) + k_i(\omega_i) - k_p(\omega_s + \omega_i)] \right\} \right\}^2 \quad (4)$$

where  $k$  denotes the wave vector of the photon and  $L$  is the length of the crystal. The plots of the pump envelope intensity  $|\alpha(\omega_s + \omega_i)|^2$ , phase matching intensity  $|\phi(\omega_s, \omega_i)|^2$  and joint spectral intensity (JSI)  $|f(\omega_s, \omega_i)|^2$  are shown in figures 1(a)–(c).

As in the analysis in [19] and [20], the width of the pump envelope intensity contour is proportional to the bandwidth of the pump, while the angle is 45 degrees in the minus direction of the horizontal coordinate because of the energy conservation law. The width of the phase matching intensity is related to the inverse of the crystal length. The angle  $\theta$  between the phase matching intensity contour and the positive direction of the horizontal coordinate, as shown in figure 1(b), is not fixed and it is decided by the group velocities of the pump ( $V_{g,p}$ ), the signal ( $V_{g,s}$ ) and the idler ( $V_{g,i}$ ). The contour of the JSI is determined by the pump envelope intensity and phase matching intensity. When the width of the pump envelope intensity and phase matching intensity are equal and the angle of the phase matching intensity is at 45 degrees, the JSI can achieve a circular shape and maximum spectral purity.

The spectral purity is a parameter which describes the degree of the spectral uncorrelation between the signal and the idler photons. It is defined as  $P = \text{Tr}(\hat{\rho}_s^2) = \text{Tr}(\hat{\rho}_i^2)$ , where  $\hat{\rho}_s$  and  $\hat{\rho}_i$  are the reduced density operators of the signal and the idler, and  $\text{Tr}$  denotes a trace acting over the matrix. This purity is decided by the factorability of the JSA and it can be calculated numerically using a method called Schmidt decomposition [21]. Schmidt decomposition entails expressing the joint spectral amplitude in terms of complete basis sets of biorthogonal vectors  $u_n(\omega_s)$  and  $v_n(\omega_i)$  such that:

$$f(\omega_s, \omega_i) = \sum_n \lambda_n u_n(\omega_s) v_n(\omega_i), \quad (5)$$

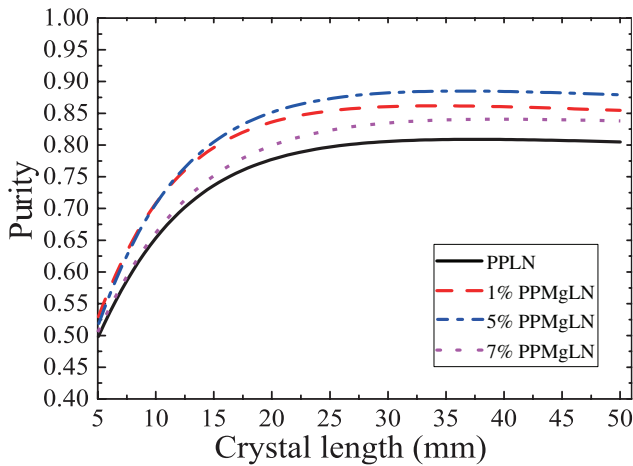


**Figure 2.** Variation of spectral purity for PPMgLN and PPLN of crystal length with a 800 nm and 600 GHz pump.

where the values  $\lambda_n$  are known as the Schmidt coefficients and  $\sum_n \lambda_n^2 = 1$ . The entanglement of the spectrum can be conveniently quantified by the Schmidt number  $K$  and it indicates the number of Schmidt modes existing between the signal and the idler photons. According to [22], the Schmidt number  $K$  is defined as

$$K = \frac{1}{\sum_n \lambda_n^4}. \quad (6)$$

The value  $K = 1$  represents a state in which there is only a single pair of active Schmidt mode functions and therefore exhibits no spectral correlation. The spectral purity of the photon pairs equals to the inverse of the Schmidt number  $K$ :

$$P = \frac{1}{K} = \sum_n \lambda_n^4. \quad (7)$$

Schmidt decomposition is useful in numerical simulation to acquire the spectral purity.

### 3. Calculation results

The purity of the photon pairs is associated with the parameters of the laser source and crystal according to the theoretical analysis in section 2. The efficiency of the SPDC is also determined by the crystal length. Therefore, it is crucial to choose the appropriate crystal length in the SPDC process. The dependence of the purity on crystal length is shown in figure 2 for PPLN and PPMgLN. In this plot, the pump wavelength is set to 800 nm and the pump bandwidth is 600 GHz.

The plot in figure 2 shows that the spectral purity of the photon pairs varies with the length of the crystal from 5 mm to 50 mm. As the formula of the intensity expression [23], the intensity of the generated photon pairs is proportional to  $\text{sinc}^2\left(\frac{\Delta k \cdot L}{2}\right)$ . Thus, the bandwidths of the signal and idler photons generated in nonlinear materials gradually become narrower with the increase in the crystal length. In this process, the divergence in frequency between the signal and idler

photons becomes harder to distinguish. The direct expression in figure 2 is the growth of the spectral purity with the crystal length from 5 mm to 25 mm. Then the spectral purity curve will flatten out gently, since the influence of the crystal length will become small when it exceeds 25 mm. Therefore, the numerical simulation we take can decide the crystal length, which is common and accords with the experiment's requirement. In this thesis, we confirm the crystal length of PPLN and PPMgLN 30 mm.

In accordance with the analysis in section 2, the contour of the JSI is determined by the pump envelope intensity and phase matching intensity, as in the examples shown in figure 1. The tilting angle of the pump envelope intensity is fixed at 45 degrees in the minus direction of the horizontal coordinate and the width of the contour relates to the pump bandwidth. Meanwhile, the angle of phase matching intensity is decided by the group velocities of the signal, the idler and the pump, which depend on the pump wavelength. We choose the crystal length of 30 mm to fix the width of the phase matching intensity. All of these analyses come to the conclusion that the pump wavelength and bandwidth have vital impacts on the JSI, as shown in figure 3. In the numerical simulation it is difficult to calculate the spectral purity of the signal and idler photons directly in the JSI. Therefore, the Schmidt decomposition is applied to analyse the spectral purity. The calculation results about the spectral purity related to the pump wavelength and pump bandwidth are indicated in figures 4(a) and (b), respectively.

In figure 4(a), the crystal length is set to 30 mm and the pump bandwidth is fixed at 600 GHz. Under these conditions, the spectral purity has a very sharp growth trend when the pump wavelength changes from 600 nm to 800 nm. When expanding the pump wavelength, the angle in figure 1(b) will change from obtuse to acute and the plot of the JSI gradually closes to a circle, as shown in figure 3. As a consequence, the spectral correlation will be reduced well. Note that although the purities do not reach one for PPLN and PPMgLN, they tend to more than 80%. The relationship between the spectral purity and the pump bandwidth are indicated in figure 4(b). In figure 4(b) the crystal length is assumed to be 30 mm and the pump wavelength is set to 800 nm. The influence of the pump bandwidth on the spectral purity is reflected in the width of the pump envelope intensity. As mentioned in the theoretical part, when the width of the pump envelope intensity and phase matching intensity are equal, the spectral purity can achieve the maximum value. Since the crystal length is fixed, the width of the phase matching intensity which relates to it is also unchanged. In the numerical simulation, we set the pump bandwidth from 10 GHz to 600 GHz. Meanwhile, the width of the phase matching intensity gradually closes to the width of the phase matching intensity. This is the reason why the spectral purity shows an increasing trend with the increase in the pump bandwidth in figure 4(b). When the pump wavelength is 800 nm and the bandwidth is 600 GHz, the results of the numerical simulation predict the spectral purity of photon pairs produced by PPLN, 1%, 5%, 7% PPMgLN are 81%, 86%, 88% and 84%, respectively. The simulation results carried out in figures 2 and 4 illustrate that the frequency correlations

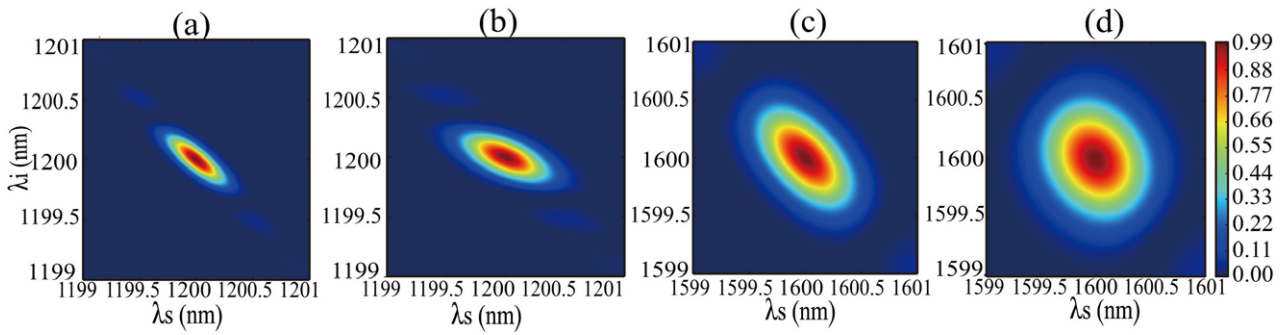


**Figure 3.** The JSI of the down-converted photons from PPMgLN (5% MgO doped) crystal. The crystal length is fixed at 30 mm. The horizontal and vertical represent the wavelength of the signal and idler photons, respectively. The pump wavelength is set to 600 nm in (a) and (b), and 800 nm in (c) and (d). In (a) and (c) the pump bandwidth is assumed to be 200 GHz and it is modified to 600 GHz in (b) and (d).

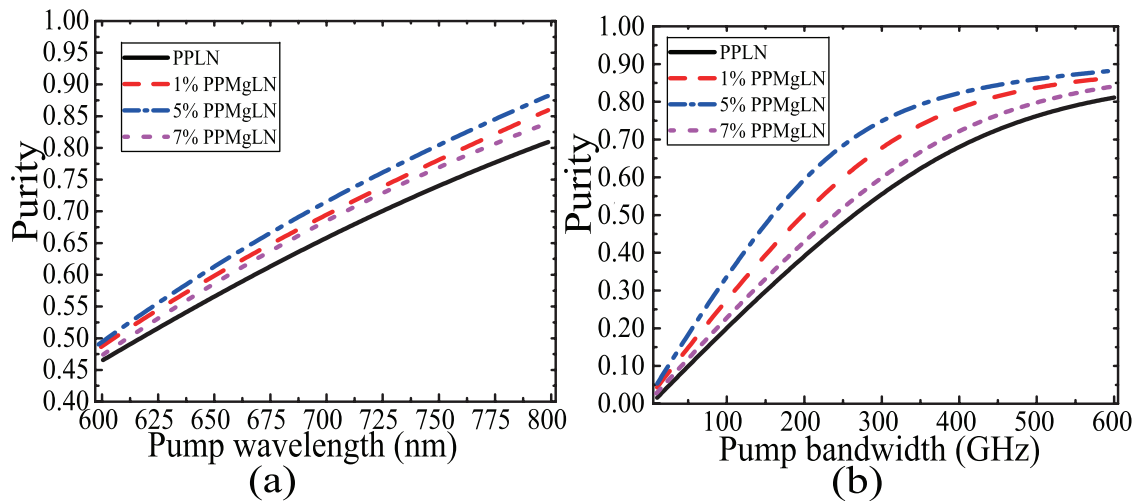


**Figure 4.** (a): The spectral purity of PPMgLN and PPLN vary with the pump wavelength from 600 nm to 800 nm. The pump bandwidth is fixed at 600 GHz and the crystal length is set to 3 cm. (b): The spectral purity of PPMgLN and PPLN with the change of the pump bandwidth from 10 GHz to 600 GHz. The pump wavelength is 800 nm and the crystal length is 3 cm.

can be reduced well with the suitable crystal length and the parameters of the pump in PPLN and PPMgLN.

As shown above, the spectral purity is not only determined by the crystal length, pump wavelength and pump bandwidth, but it is also influenced by the doping concentration of the nonlinear materials. The doping concentration will change the nonlinear optical characters of the crystal, which causes the difference of the spectral purity under the same conditions. The plots in figures 2 and 4 indicate that the PPMgLN is an excellent choice to generate pure photon pairs which are suitable for a communication band. The pump wavelength and the pump frequency have a positive influence on spectral purity and we can obtain high spectral purity photon pairs by adjusting the parameters of the crystal and the pump source. A comparison of PPLN and PPMgLN with different doping concentrations allows us to come to the conclusion that the purity of the photon pairs is closely related to the doping concentration. 5% PPMgLN is the best one for generation of spectral uncorrelated photon pairs.

#### 4. Conclusion

In this paper, we propose a method for generating pure indistinguishable photon pairs at telecom wavelength by SPDC in

PPLN and PPMgLN. We show that the spectral correlation can be reduced only by adapting the spectrum of pump pulses and the dispersion property of the nonlinear crystal without using narrow filters. We obtain a spectral purity of more than 84% in MgO doped PPLN by the numerical simulation. Therefore, it is a preferable choice for minimising the correlation in frequency between signal photons and idler photons at telecom wavelength. These nonlinear materials and the technique proposed may provide useful tools for the management of spectral uncorrelated photon pairs in quantum communication and networking.

#### Acknowledgments

This work was supported in part by the National Natural Science Foundation of China under Grant Nos. 61125503 and 61235009, and the Foundation for Development of Science and Technology of Shanghai under Grant No. 13JC1408300.

#### References

- [1] Bouwmeester D, Mattle K, Pan J W, Weinfurter H, Zeilinger A and Zukowski M 1998 *Appl. Phys. B* **67** 749

- [2] Pan J W, Bouwmeester D, Weinfurter H and Zeilinger A 1998 *Phys. Rev. Lett.* **80** 3891
- [3] Gisin N and Thew R 2007 *Nat. Photon.* **1** 165
- [4] Gisin N, Pironio S and Sangouard N 2010 *Phys. Rev. Lett.* **105** 070501
- [5] Kwiat P G, Mattle K, Weinfurter H, Zeilinger A, Sergienko A V and Shih Y 1995 *Phys. Rev. Lett.* **75** 4337
- [6] Steinlechner F, Ramelow S, Jofre M, Gilaberte M, Jennewein T, Torres P J, Mitchell M W and Pruneri V 2013 *Opt. Express* **21** 11943
- [7] Kim Y H, Chekhova M V, Kulik S P, Rubin M H and Shih Y 2001 *Phys. Rev. A* **63** 062301
- [8] Laiho K, Cassemiro K N and Silberhorn C 2009 *Opt. Express* **17** 22823
- [9] Tanzilli S, Riedmatten H D, Tittel W, Zbinden H, Baldi P, Micheli M D, Ostrowsky D B, Gisin N 2001 *Electron. Lett.* **37** 26
- [10] Grice W P, U'Ren A B and Walmsley I A 2001 *Phys. Rev. A* **64** 063815
- [11] Zukowski M, Zeilinger A and Weinfurter H 1995 *Ann. NY Acad. Sci.* **755** 91
- [12] Halder M, Beveratos A, Gisin N, Scarani V, Simon C and Zbinden H 2007 *Nat. Phys.* **3** 692
- [13] Fulconis J, Alibart O, O'Brien J L, Wadsworth W J and Rarity J G 2007 *Phys. Rev. Lett.* **99** 120501
- [14] Gerrits T et al 2011 *Opt. Express* **19** 24434
- [15] Bruno N, Martin A, Guerreiro T, Sanguinetti B and Thew R T 2014 *Opt. Express* **22** 17246
- [16] Lim H C, Yoshizawa A, Tsuchida H and Kikuchi K 2008 *Opt. Express* **16** 12460
- [17] Kaiser F, Issautier A, Ngah L A, Danila O, Herrmann H, Sohler W, Martin A and Tanzilli S 2012 *New J. Phys.* **14** 085015
- [18] Gayer O, Sacks Z, Galun E and Arie A 2008 *Appl. Phys. B* **91** 343
- [19] Edamatsu K, Shimizu R, Ueno W, Jin R B, Kaneda F, Yabuno M, Suzuki H, Nagano S, Syouji A and Suizu K 2011 *Prog. Inform.* **8** 19
- [20] Jin R B, Shimizu R, Wakui K, Benichi H and Sasaki M 2013 *Opt. Express* **21** 10659
- [21] Law C K, Walmsley I A and Eberly J H 2000 *Phys. Rev. Lett.* **84** 5304
- [22] Eberly J H 2006 *Laser Phys.* **16** 921
- [23] Boyd R W 2003 *Nonlinear Optics* (New York: Academic)